Chinese Journal of Polymer Science Vol. 35, No. 7, (2017), 809–822

Chinese Journal of Polymer Science
© Chinese Chemical Society
Institute of Chemistry, CAS
Springer-Verlag Berlin Heidelberg 2017

Excellent Hydrophilic and Anti-bacterial Fouling PVDF Membrane Based on Ag Nanoparticle Self-assembled PCBMA Polymer Brush*

Jian-hua Li**, De-bin Zhang, Xing-xing Ni, Hui Zheng and Qi-qing Zhang**
Institute of Biomedical and Pharmaceutical Technology, Fuzhou University, Fuzhou 350001, China

Abstract A silver nanoparticles-poly(carboxybetaine methacrylate) (AgNPs-PCBMA) nanocomposite was prepared on poly(vinylidene fluoride) (PVDF) membrane surface to improve its hydrophilicity and antifouling properties. Firstly, the PVDF membranes were grafted by PCBMA *via* physisorbed free radical grafting technique. Then Ag^+ coordinated to the carbonyl group on PCBMA and subsequently was reduced to silver nanoparticles. The hydrophilicity of the PVDF-*g*-PCBMA/Ag membrane was enhanced with the increasing fixed degree (FD) of AgNPs, and the original water contact angle of membrane was reduced to 33.97°. Additionally, water flux recovery ratio (FRR) and bovine serum albumin (BSA) rejection ratio of PVDF-*g*-PCBMA/AgNPs membrane were improved from 52% to 93.32% and 28.12% to 91.12%, respectively. Further, the PVDF-*g*-PCBMA/AgNPs membranes exhibited the more pronounced inhibition zone. The study demonstrated that compared with pure AgNPs or the PCBMA polymer brush, the synergistic effect of PCBMA and AgNPs made PVDF membranes have better hydrophilicity and anti-bacterial performances.

Keywords PVDF membrane; Zwitterionic monomer CBMA; Silver nanoparticle; Antifouling performance; Antibacterial ability

INTRODUCTION

As a popular polymer membrane material, poly(vinylidene fluoride) (PVDF) has been received a great deal of attention because of its outstanding chemical resistance, thermal stability and mechanical properties[1–3]. However, using PVDF membrane in water treatment is restricted due to its hydrophobicity characteristic, which often causes severe membrane fouling[4–6]. Among them, organic fouling and bio-fouling are the main pollution of the membrane. Organic fouling is often caused by protein adsorption on surface and in pores of membranes. Thus, surface hydrophilic modification is a useful strategy to improve the anti-organic fouling ability of PVDF membranes[7–13]. However, for bio-fouling, the adsorption and growth of bacteria on the membrane surface will lead to pore blocking. Hence, we need a novel membrane which possesses not only hydrophilicity but also excellent antibacterial activity at the same time to endow the superior anti-bio-fouling performance.

Recently, the inorganic antibacterial materials silver nanoparticles (AgNPs) were widely used for preparing anti-bio-fouling separation membrane[14–21] due to their effectiveness against various aquatic microorganisms including bacteria, fungi, algae, *etc*[22, 23]. To introduce AgNPs on membrane, two common methods can be feasible: blending and surface immobilization. Shi *et al.* introduced Ag-self-assembled NaY zeolites into hollow fiber PVDF membrane *via* the blending method, and the results confirmed that the novel nanoparticles endowed

* This work was financially supported by the National Natural Science Foundation of China (Nos. 51303028 and 31401609) and Test Fund support by Test Center of Fuzhou University.
** Corresponding authors: Jian-hua Li (李建华), E-mail: jhli_2005@163.com
Qi-qing Zhang (张其清), E-mail: zhangqiq@126.com
Received December 15, 2016; Revised February 13, 2017; Accepted March 2, 2017
doi: 10.1007/s10118-017-1944-3

PVDF membrane excellent antibacterial property[19]. Chen *et al.* also prepared an effective anti-bio-fouling polyethersulfone (PES) membrane also *via* blending with halloysite nanotubes-chitosan-Ag nanoparticles (HNTs-CS@Ag) and the compatibility between nanoparticles and membrane was enhanced[20]. The AgNPs blended membranes could have some antibacterial effect, but a large portion of the particles could not play its proper role as the AgNPs were embedded in the membrane[14–17]. In addition, the poor compatibility between nanoparticles and organic membrane could not ensure that less number of AgNPs or Ag^+ ions released into water[18]. Therefore, many researchers have been trying to solve this problem *via* immobilizing the AgNPs to an organic or inorganic carrier[19–24]. Li *et al.* prepared a Ag/poly(vinylidene fluoride)-*g*-poly(acrylic acid) (PAA) membrane by coordination between Ag^+ and the carbonyl group of PAA and investigated the influence of silver ion concentration on the antifouling performance of membranes[23]. Yin *et al.* grafted AgNPs on thiol-terminated membrane surface *via* the Ag—S chemical bonding to obtain a higher water flux and an anti-bio-fouling membrane[24]. Previous researches were mainly focused on application of silver nanoparticles in membrane fabrication and the connecting bridge only played the role of immobilization. The bridge with hydrophilic or anti-bacterial capability has seldom been reported.

The modified membrane with zwitterionic polymer poly(carboxybetaine methacrylate) (PCBMA) was recently studied due to its high hydration capacity and excellent anti-bacterial ability[25, 26]. Cheng *et al*. prepared a zwitterionic PCBMA polymer brush film *via* atom transfer radical polymerization (ATRP) and investigated the anti-bacterial fouling property[27]. Their results demonstrated that the PCBMA grafted surfaces possessed a long-term anti-bacterial ability at different temperatures. Hu *et al.* reported silver-zwitterion nanocomposite on glass chips to get the superior antimicrobial and anti-adhesive capabilities[28]. But the mechanism of the synergistic effect of AgNPs and the zwitterionic polymer brush on the enhancement of hydrophilic and antimicrobial capabilities has not been discussed. Further, this method applied to the membrane has not been reported yet.

In this work, we combined zwitterionic CBMA with AgNPs to improve the anti-organic fouling and anti-bio-fouling properties of PVDF membrane. Initially, the PVDF membrane surface was grafted by PCBMA *via* physisorbed free radical grafting technique which was first used and proved in the grafting modification of PVDF membrane by our group[29]. Then Ag^+ coordinated to the carbonyl group from PCBMA and subsequently reduced to silver nanoparticles, resulting in different amounts of AgNPs fixed to the membrane. In this strategy, the zwitterionic PCBMA not only played a role of bridge to connect AgNPs with membrane but improved the antifouling capability of the membrane. We demonstrated that the antifouling ability of PVDF membrane was greatly enhanced due to synergistic effect of AgNPs and the zwitterionic PCBMA polymer brush on membranes.

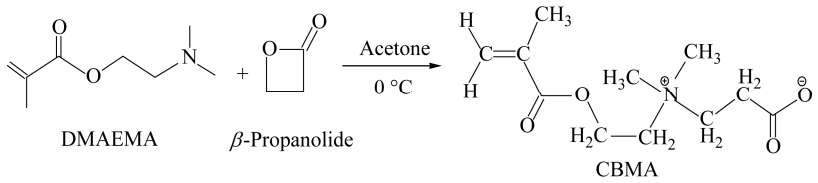
EXPERIMENTAL

Materials and Reagents

2-(*N*,*N*′-dimethylamino) ethyl methacrylate (DMAEMA, 98%), *β*-propiolactone (95%), polyvinylpyrrolidone (PVP), silver nitrate ($AgNO_3$), 2,2′-azobisisobutyronitrile (AIBN), sodium borohydride ($NaBH_4$), DMAc and anhydrous acetone were purchased from Sigma-Aldrich. PVDF (FR-904) ($M_n = 3.8 \times 10^5$) was obtained from Shanghai 3F New Materials Co., Ltd. and was dried at 80 °C for 12 h before use. Acrylic acid (AA) was obtained from Merck Company. Bovine serum albumin (BSA, $M_n = 6.7 \times 10^4$ Da) was obtained from Aldrich Chemical Co., Ltd. and used as received.

Synthesis of CBMA Monomer

Carboxybetaine methacrylate (CBMA) was synthesized by the reaction of DMAEMA and *β*-propiolactone referring to a method published previously[30] and the yield reached 92.7% as we used an ice bath (Scheme 1). The detailed steps were as follows: DMAEMA (1.57 g, 10 mmol), *β*-propiolactone (0.87 g, 12 mmol), and anhydrous acetone with water removed by molecular sieve (50 mL), were added into a 100 mL round-bottom flask with a magnetic stirrer and an argon inlet. The system was maintained at 0 °C for 6 h in an argon atmosphere and then a white precipitate was gradually obtained. The product was filtered, then washed by anhydrous acetone, followed by absolute ethyl alcohol for three times. Finally, the whiter solid was dried at room temperature under high vacuum and kept in the refrigerator in 4 °C.



Scheme 1 Synthesis and chemical structure of CBMA

Preparation of Original PVDF Membrane

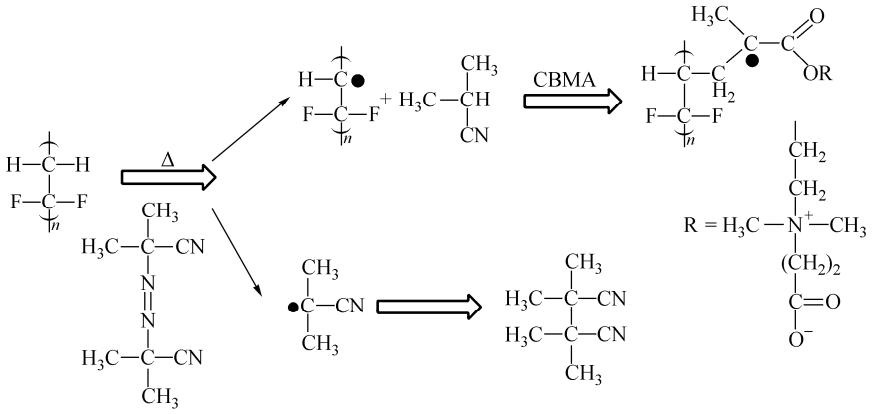
The original PVDF membranes were prepared *via* the classical non-solvent induced phase separation process (NIPS). PVDF powder and PVP were added into DMAc solution according to the compositions listed in Table 1, and stirred and dissolved completely at 65 °C. After degassing for 2 h, the solution was cast on the nonwovens and spread with a 200 μm-thick steel knife and then immersed into a water coagulation bath. Finally, the membranes were washed with deionized water for three days and dried at room temperature. The original PVDF membrane was denoted as M0.

Table 1 Composition of the membranes

Membranes	PVDF (wt%)	PVP (wt%)	DMAc (wt%)	*g*-PCBMA (mg/cm^2)	The concentration of $AgNO_3$ solution (mL/L)
M0	15	3	82	0	0
M1	15	3	82	1.63	0
M2	15	3	82	1.63	0.01
M3	15	3	82	1.63	0.05
M4	15	3	82	1.63	0.1

Preparation of the PVDF-g-PCBMA Membrane

The strategy of grafting zwitterionic PCBMA on PVDF membrane *via* physisorbed free radical polymerization method was firstly used in the PVDF membrane modification by our group[29]. The reaction mechanism of surface grafted free radical polymerization is shown in Scheme 2. The detailed steps were described as follows.



Scheme 2 Mechanism of synthesis of PVDF-*g*-PCBMA

Three pieces of the PVDF membranes (3 cm × 3 cm) were immersed into acetone-AIBN solution (10% AIBN, *W*/*W*) for 30 min and dried in vacuum at 30 °C. Then the membranes were placed into a round bottom flask with 3 g of CBMA in 30 mL of methanol and water (30/70, *W*/*W*) mixture. After purging with nitrogen for 30 min, the reaction was carried out in oil bath at 70 °C for 5 h. The membranes were washed with water for several times. After dried in air, the samples were stored in a desiccator before used. For the purpose of a contrast analysis, the PVDF-*g*-PAA membrane was prepared under a similar procedure. The grafted density (GD) was calculated gravimetrically according to the following equation:

$$GD\ (mg/cm^2) = (W_1 - W_0)/A_m \quad (1)$$

where W_1 denotes the weight of PVDF membrane after the grafting and W_0 is the initial PVDF membrane weight. A_m is the area of the membrane. The PVDF-*g*-PCBMA membrane was named as M1 in this paper.

Preparation of PVDF-g-PCBMA/Ag Membrane

The PVDF-*g*-PCBMA membrane with the grafted density of 1.63 mg/cm^2 was selected for preparing PVDF-*g*-PCBMA/Ag membranes. In the PCBMA brushes, COOH groups existed as carboxylic groups (COO^-) which neutralized the zwitterion with positively charged quaternary ammonium ion. Ag^+ was easy to coordinate with the carboxylic groups (COO^-) with two oxygen atoms which had two pairs of lone pairs of electrons, respectively. Generally, the PVDF-*g*-PCBMA membrane was soaked in a freshly prepared solution of $AgNO_3$ (0.01, 0.05 and 0.1 mL/L, Ag^+) and stirred in the dark for 0.5 h. Then the membrane was put into $NaBH_4$ solution of appropriate concentration and stirred in the dark for 15 min. The obtained sample was washed with water and dried in vacuum. The PVDF-*g*-PCBMA/Ag membranes were denoted as M2, M3, M4, according to different concentrations of $AgNO_3$ (Table 1). The PVDF-*g*-PAA/Ag membranes prepared by the same method were denoted as m1, m2, m3, m4. The fixed degree (FD) was calculated gravimetrically according to the following equation:

$$FD\ (mg/cm^2) = (W_2 - W_1)/A_m \quad (2)$$

where W_2 denotes the weight of PVDF membrane after the fixing reaction.

Characterization

The chemical structure of CBMA was characterized using liquid state ^1H (400 MHz) nuclear magnetic resonance (NMR) spectroscopy (Bruker 500 AVANCE III spectrometer).

The prepared membranes were investigated by attenuated total reflectance Fourier transform infrared spectroscopy (ATR-FTIR, Thermo Nicolet 360, USA).

The surface morphology of membranes was observed by scanning electronic microscopy (SEM, SIRION-100, FEI Co., Ltd.). To study the cross-sectional fracture of the membranes, the membranes were fractured and flexed into a short sample in liquid nitrogen and then were sputter-coated with gold-palladium alloy before microscopic analysis.

The chemical compositions of the prepared membrane surfaces were investigated by X-ray diffraction (XRD, X' Pert Pro MPD, NED) using Cu Kα radiation (λ = 0.15406 nm) at 40 kV and 30 mA with a scan speed of 2 (°)/min and scan range of 10°–80° and X-ray photoelectron spectroscopy (XPS, PHI 5000C ESCA system, PHI Co., USA). The X-ray source was operated under a power of 250 W (14.0 kV, 93.9 eV) with an electron takeoff angle of 90° in comparison with the sample plane.

Surface Hydrophilicity of Membrane

The hydrophilicity of membranes was characterized *via* contact angle (OCA20, Data physics, Germany). To minimize experimental error, the contact angles were measured five times for each sample and then were averaged.

Static Protein Adsorption of Membranes

The membrane was washed with phosphate buffer for 24 h to remove the active groups and pollutants on membrane surface. The sample was immersed into six test tubes with BSA solution (1 g/L) and then shaking for 24 h at room temperature (M0−M4). After attaining adsorption equilibrium, the membrane was removed and rinsed with 5 mL of phosphate buffer solution (PBS), which was added into the stoste, then the absorbance of BSA solution was measured (λ = 280 nm) for concentration determination. The BSA adsorption capacity of the membrane was calculated according to the concentration change of the BSA solution.

Ultrafiltration (UF) Experiment

The UF experiments were performed using the dead ended filtration system. Firstly, each membrane was initially compacted for about 30 min at 0.2 MPa to obtain a stable flux; then the pure water flux (J_{w1}) was measured at 0.2 MPa. The flux of 1 g/L BSA (PBS, PH = 7.4) was also measured at 0.2 MPa for 60 min, recorded as J_p.

Subsequently, the membrane was immersed in deionized water for 2 h at 20 °C and then the pure water flux (J_{w2}) was measured.

The flux (J_w and J_p) was calculated as:

$$J = \frac{V}{A\Delta t} \tag{3}$$

where J (L/(m^2·h)) is the flux, V (L) is the permeate volume, A (m^2) is the membrane effective area and Δt (h) is the time.

The water flux recovery ratio (FRR) was calculated as follow[31]:

$$\text{FRR}\ (\%) = J_{w2}/J_{w1} \times 100 \tag{4}$$

The BSA rejection ratio (R_{BSA}) was calculated by the following equation:

$$R_{BSA}\ (\%) = (1 - C_p/C_f) \times 100 \tag{5}$$

where C_p and C_f (g/L) represent BSA concentrations in permeate and feed solution, respectively.

The resistance-in-series model was used to analyze the detailed fouling of membranes and calculated as follows[32]:

$$R_t\ (\%) = (1 - J_p/J_{w1}) \times 100 \tag{6}$$

$$R_r\ (\%) = (J_{w2} - J_p)/J_{w1} \times 100 \tag{7}$$

$$R_{ir}\ (\%) = (J_{w1} - J_{w2})/J_{w1} \times 100 \tag{8}$$

where R_t means the total fouling resistance, and R_r refers to the reversible fouling resistances, R_{ir} means the irreversible fouling resistances on surface and in pores.

Durability of the Membranes

We investigated the durability of the membranes by measuring the water contact angle of the membrane surface. M1–M4 were immersed in methanol and water and leached by continuous shaking for various periods at room temperature. Each time after drying the leached membranes, the water contact angle was measured again.

Antibacterial Experiment

In the present work, *S. aureus* (ATCC100419) and *E. coli* (ATCC090401) were selected as the Gram positive and Gram negative bacterial strains model to assess the anti-bio-fouling activity of PVDF membrane by the inhibition zone method[33]. Briefly, the tested bacteria were initially incubated in a nutrient broth (NB, pH 7.4) with shaking speed of 160 r/min (37 °C, 24 h). Subsequently, the diluted bacteria solution (100 μL) was well spread on the separate NB agar culture medium. After sterilized by ultraviolet radiation for 30 min, membranes were then placed on the NB agar. After a period of 24 h cultivation, the inhibition zone around the membrane was observed as an indicator of anti-bio-fouling activity.

RESULTS AND DISCUSSION

^{1}H-NMR Spectrum of CBMA

^{1}H-NMR of CBMA was recorded on a Bruker spectrometer using deuterated water as a solvent. In Fig. 1, the results were accorded with previous reports[30]. ^{1}H-NMR (50 MHz, δ): 6.06 (s, 1H, =CH), 5.68 (s, 1H, =CH), 4.55 (t, 2H, OCH_2), 3.70 (t, 2H, CH_2N), 3.59 (t, 2H, NCH_2), 3.10 (s, 6H, NCH_3), 2.64 (t, 2H, CH_2COO), 1.84 (s, 3H, $=CCH_3$).

Mechanism of the Physisorbed Free Radical Grafting Technique

The mechanism of physisorbed free radical initiating grafting polymerization on PVDF membrane was investigated and reported preliminarily by our group[29]. AIBN was decomposed into isobutyronitrile radicals when the reaction temperature rose. For the isobutyronitrile radical, three possible reactions would occur: (1) two isobutyronitrile radical terminating each other, (2) initiation of a free radical polymerization in solution, and (3)

extraction of hydrogen from PVDF backbone (Scheme 2). The macro-radical formed from hydrogen extraction could react with CBMA in solution to form grafted polymer chains. Energetically, the extraction of the hydrogen from the surface of the PVDF membrane was unfavorable. However, at the interphase of solid and liquid solution, the reaction of isobutyronitrile radicals and PVDF could be enhanced by the lack of diffusion of the initiator radicals into the aqueous environment[34].

In order to investigate how the AIBN radicals interacted with the PVDF surface, several PVDF membranes containing AIBN were placed into a round bottom flask with the same polymerization conditions, excluding the CBMA monomer. The mixture was evaporated by a rotary evaporator after the reaction. The ^{1}H-NMR was used to analyze the residue. In the ^{1}H-NMR result (Fig. 2), the peaks at δ = 2.4 and 1.02 were attributed to the methyl hydrogens of the hydrogen capped product, with the integration equal to 1:6. The other single at δ = 1.26 was indicative of the combination byproduct[29]. From the results of ^{1}H-NMR, the reaction route of Scheme 2 may be confirmed basically.

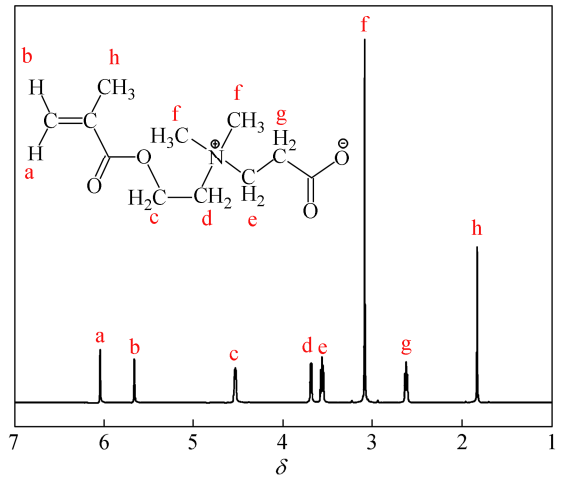


Fig. 1 ^{1}H-NMR spectrum of zwitterionic monomer CBMA (D_2O)

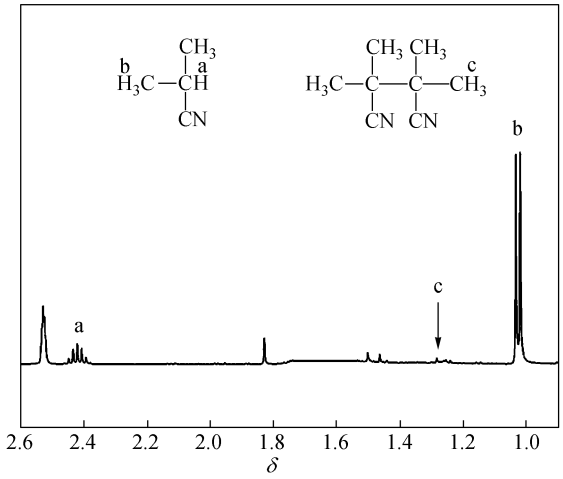


Fig. 2 ^{1}H-NMR spectrum of hydrogen capped AIBN radicals (DMSO-d_6)

The FTIR measurement was used to characterize hydrogen capped AIBN radicals. In Fig. 3, the peaks at 2876, 2238 and 1364 cm^{-1} were corresponding to the C—H, C—N and gem-dimethyl (CH_3—C—CH_3), respectively. The FTIR result confirmed that surface initiated grafting polymerization on PVDF membrane using

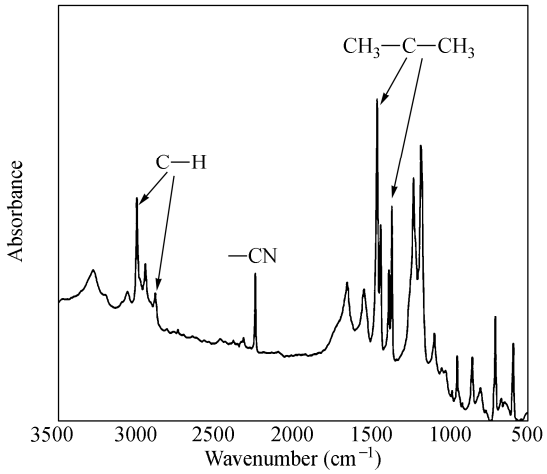


Fig. 3 FTIR spectrum of hydrogen capped AIBN radicals

AIBN as the initiator would be mainly on account of the extraction of hydrogen from the PVDF backbone. Hence, the PCBMA chains could be directly attached to the PVDF backbone and retained its original nature in this graft process. This method would maintain the integrity of the main-chain structure of PVDF and thus well preserve its excellent physical properties.

Characterizations of the PVDF-g-PCBMA/Ag Membranes

FD of the membranes

The relationship between Ag^+ concentration and FD is shown in Fig. 4(a). The FD increased with the growing concentration and reached 32.78 mg/cm^2 at the concentration of 0.1 g/mL. As shown in Fig. 4(b), the apparent color of the modified membranes deepened with the increasing concentration of Ag^+ ions. These results suggested that the immobilization strategy was efficient and a few PCBMA brushes could load a large number of AgNPs by covalent bond on membrane surface.

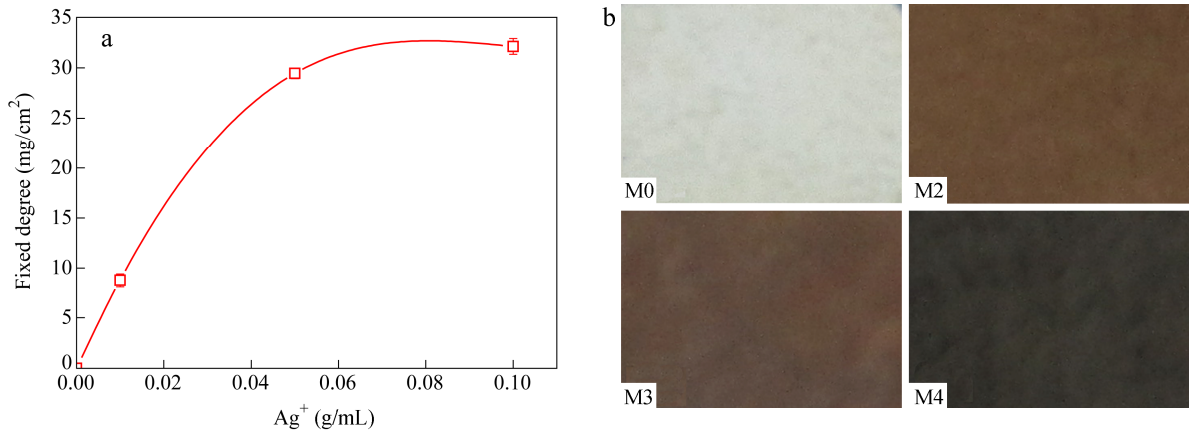


Fig. 4 (a) The fixed degree (FD) of AgNPs and (b) membrane images with different concentration of Ag^+ ion in solution

FTIR-ATR characterizations of the membrane

The result of FTIR-ATR is shown in Fig. 5 and the new absorption band appearing at the wavenumber of 1722 cm^{-1} was correlated to the stretching vibration of carboxyl group (—C=O) from the PCBMA polymer chains on the PVDF-*g*-PCBMA membrane (M1). The comparisons demonstrated that the CBMA grafted reaction was successful. The band at 1660 cm^{-1} around belonged to the amide bond of the residual PVP as a pore forming agent in this work[11].

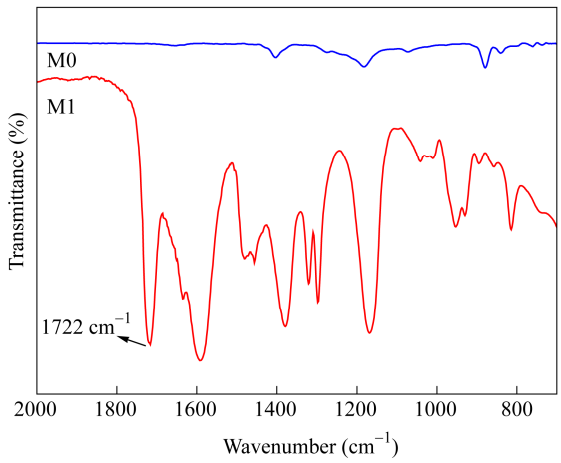


Fig. 5 ATR-FTIR spectra of pure PVDF membrane (M0) and PVDF-*g*-PCBMA membrane (M1)

Morphology of membranes

Morphology of the membranes was investigated by SEM, as shown in Fig. 6. Owing to large crystallization areas appearing in non-solvent induced phase separation (NIPS) process, many white dots existed on the surface of the original PVDF membranes (M0). It could be seen that the white dots blurred gradually from M0 to M1, confirming that PCBMA brushes had grafted onto membrane successfully. Such conclusion could be inferred from the cross section of the original (M0-1) and PVDF-*g*-PCBMA membranes (M1-1) which became rougher due to the presence of the PCBMA brushes. This also indicated that graft polymerization occurred both on the surface and pore wall. Compared with M0, the pore density of modified membranes gradually decreased and surfaces became rougher with increasing silver ion concentration. Additionally, it could be seen clearly that the AgNPs appeared on the membrane surface and the quantity increased with increasing silver ion concentration. The AgNPs-PCBMA brushes were evidently observed on the membrane surface of M2. As for M3 and M4, the amount of AgNPs immobilized on the membrane surface gradually increased. The changes of membrane morphology might have a profound impact on hydrophilicity and antifouling property of membranes.

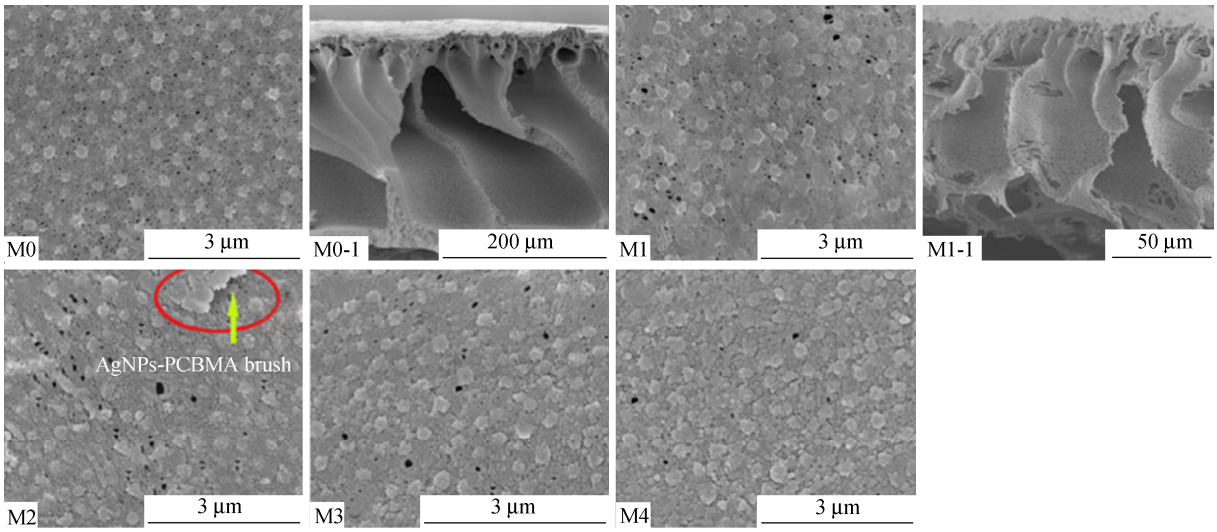


Fig. 6 SEM images of pure PVDF membrane surface (M0) and cross section (M0-1), PVDF-*g*-PCBMA membrane surface (M1) and cross section (M1-1), and PVDF-*g*-PCBMA/Ag membrane surface (M2–M4)

XRD analysis

As shown in Fig. 7, the diffraction peaks of Ag (200) appeared in the XRD curves and had higher intensity with

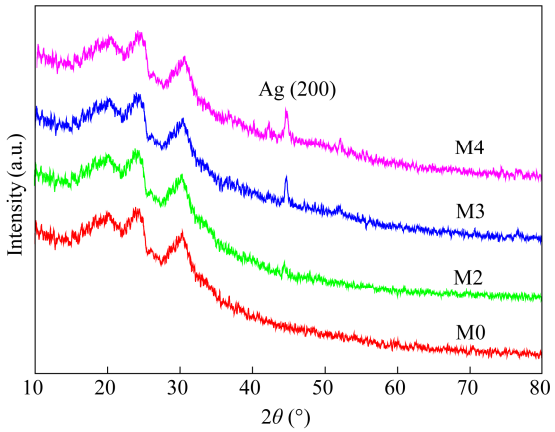


Fig. 7 XRD patterns of pure PVDF membrane (M0), and PVDF-*g*-PCBMA/Ag membranes (M2–M4)

the increase of concentration of silver nitrate. The new peaks indicated that the PCBMA polymer-brush fixed silver NPs on the membrane surface. In the solution, the positively charged silver ions (Ag^+) were attracted by the negatively charged carboxyl groups ($-COO^-$) due to the electrostatic attraction. The amount of self-assembled AgNPs increased with the increase of the concentration of silver ions (Ag^+).

XPS analysis

The existence of silver NPs on membrane surface (M4) was analyzed *via* XPS compared with PVDF membrane (M0) and PVDF-*g*-PCBMA membrane (M1). As shown in Fig. 8, only C and F binding energies (BE) were observed in the survey spectrum of pure PVDF membrane, corresponding to the C1s (289.39 eV) and the F1s (686.51 eV) for PVDF. For PVDF-*g*-PCBMA membrane, two new peaks appeared at 533.01 eV for the O1s and 397.40 eV for the N1s, respectively. As to PVDF-*g*-PCBMA/Ag membranes, a new peak located at 370.2 eV corresponding to Ag3d, which suggested that the AgNPs had been fixed on membrane surface by CBMA polymer-brush.

The C1s core level spectra of XPS were resolved into several peaks representing different chemical environments of membranes (Figs. 8b and 8c). As pure PVDF membrane, C1s core-level spectrum was curve-fitted with three peak components, with binding energies (BEs) at 284.60 eV for the neutral $-CH$ species, 285.82 eV for the $-CH_2$ species and 290.5 eV for the $-CF_2$ species consistent with the chemical structure of PVDF. The five C1s peak components of PVDF-*g*-PCBMA/Ag membrane were observed, the PVDF main chains with BE at 284.65 eV for the $-CH$, 285.80 eV for the $-CH_2$ (PVDF) and 290.5 eV for the $-CF_2$

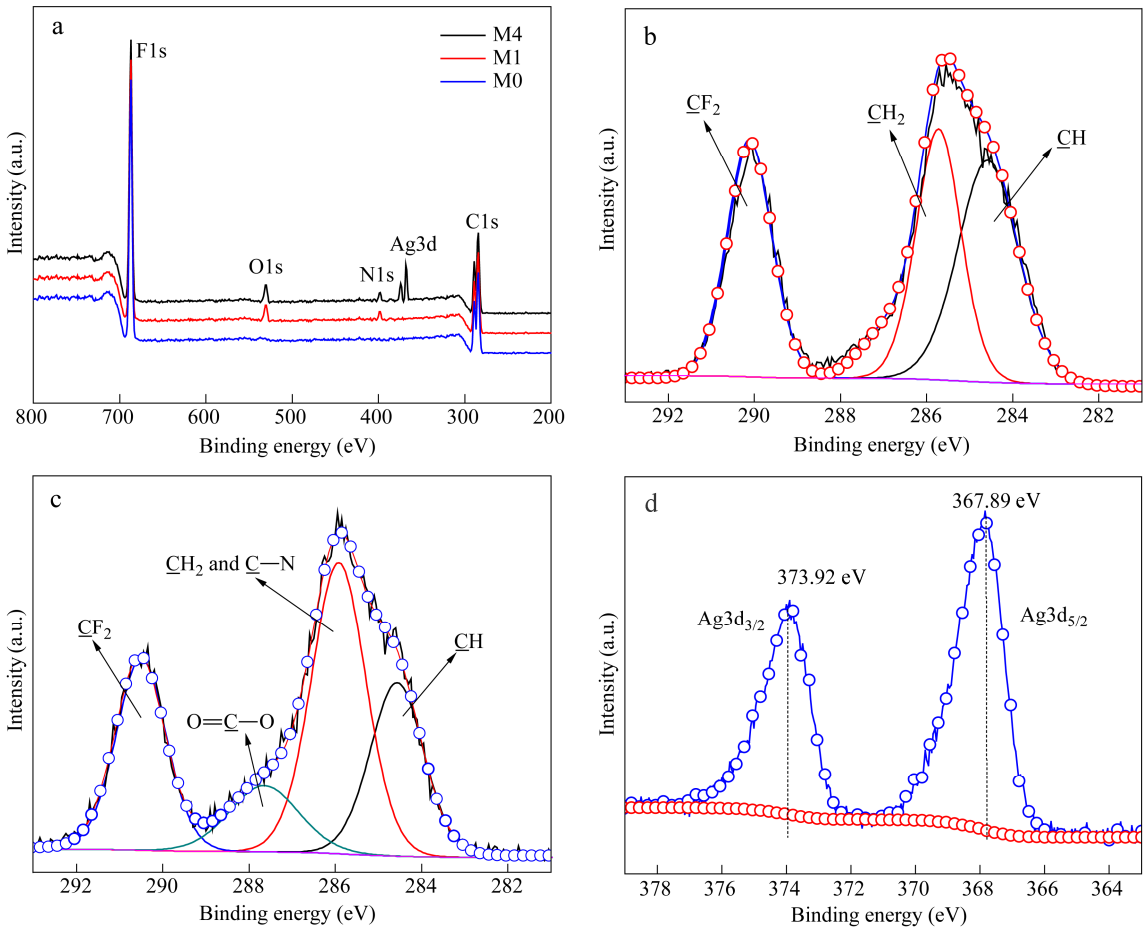


Fig. 8 (a) XPS spectra of pure PVDF membrane (M0), PVDF-*g*-PCBMA membrane (M1) and PVDF-*g*-PCBMA/Ag membranes (M4); (b, c) C1s XPS spectra of M0 and M4, respectively; (d) XPS spectrum of Ag3d (M4)

species. The peaks at 286.27 eV and 286.7 eV were assigned to the —C—N and —COO^- species of CBMA. The intensity of —CH bond at 284.60 eV from CBMA enhanced significantly with the [—CH]:[—CH_2] peak component area ratio of about 1:1. The detailed two peaks of Ag3d, $Ag3d_{5/2}$ (BE, 367.89 eV) and $Ag3d_{3/2}$ (BE, 373.92 eV) are shown in Fig. 8(d). Thus, combination of XPS with XRD and ATR-FTIR analysis undoubtedly demonstrated that the AgNPs had fixed to the membrane successfully.

Synergistic Effect of the PCBMA Polymer Brush and AgNPs on the Membrane Surface Hydrophilicity

Water contact angle measurement is an accepted way to investigate the membrane surface hydrophilicity[35]. The results of water contact angle are shown in Fig. 9. The PVDF-*g*-PCBMA membrane (M1) showed smaller contact angle than that of the pure PVDF membrane (M0) due to the hydrophilicity of PCBMA brush. After fixed AgNPs, the contact angle of the membrane decreased from 76.12° to 58.07° (M2), 48.31° (M3), 33.97° (M4) with the increasing amount of silver ion in solution. The water contact angle of the PVDF-*g*-PAA/Ag membrane with the same FD of AgNPs was 51.82° and far above the water contact angle of the PVDF-*g*-PCBMA/Ag membrane. The result not only demonstrated that AgNPs had a contribution to the hydrophilicity of the membrane, but also showed that the PCBMA polymer brush and AgNPs had a synergistic effect in terms of hydrophilic property.

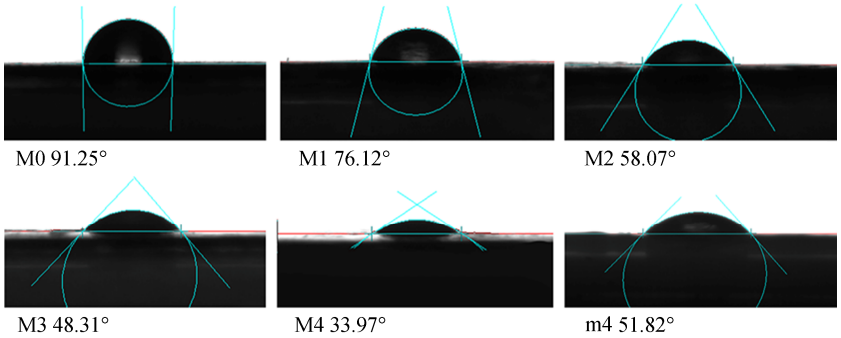


Fig. 9 The initial water contact angles of pure PVDF membrane (M0), PVDF-*g*-PCBMA membrane (M1), PVDF-*g*-PCBMA/Ag membranes (M2–M4) and PVDF-*g*-PAA/Ag membrane (m4)

The possible mechanism of how the synergistic effect of AgNPs and the zwitterionic PCBMA polymer brush enhanced the hydrophilicity of the membrane was proposed as follows. Firstly, the positively charged ammonium groups and negatively charged carboxyl groups of PCBMA could form hydrogen bonds with water molecules to produce the surface hydrophilic layer for enhancing the hydrophilicity of the membrane[25, 26]. Secondly, a large number of hydrophilic silver ions were released into water during the oxidation reaction between AgNPs and O_2 in an aqueous medium and then adsorbed on the surface of AgNPs, in the formation of a hydrated silver ion which was the probable source of silver nanoparticles hydrophilicity[23]. This result further enhanced the hydrophilicity of the membrane. Moreover, according to the mechanism of silver ion release, silver ion release rates had been demonstrated to increase with decreasing pH during the oxidation release process of silver[36]. In this study, the zwitterionic PCBMA polymer brush had at least three functions: first, to form a hydrophilic layer on the membrane surface by electrostatic interactions with water molecules; second, to provide a fixation site for silver nanoparticles; third, to create a relatively low pH conditions for silver ion release. Thus, through the synergistic effect of AgNPs and the zwitterionic PCBMA polymer brush, the AgNPs-PCBMA layer endowed the PVDF membranes a more hydrophilic surface than the results reported in other papers[23, 24].

BSA Static Adsorption of Membranes

Bovine serum albumin (BSA) is usually used to evaluate the antifouling ability of separation membranes[37]. This study selected five samples including pristine PVDF membrane and PVDF-*g*-PCBMA/Ag membranes. As can be seen from Fig. 10, the BSA adsorption of PVDF-*g*-PCBMA/Ag membranes was much lower than that of the pristine PVDF, and the difference became increasingly apparent with the increase of Ag nanoparticles. In the

1 g/mL BSA solution, the protein deposited on the original PVDF membrane was about 752 μg/cm^2. But the protein amount on the PVDF-*g*-PCBMA/Ag membranes decreased by degrees and reduced to 361, 278 and 182 μg/cm^2, respectively. These results suggested that the PVDF-*g*-PCBMA/Ag membranes obtained had good antifouling performance, which was also enhanced as the Ag nanoparticles existed on the membrane surface.

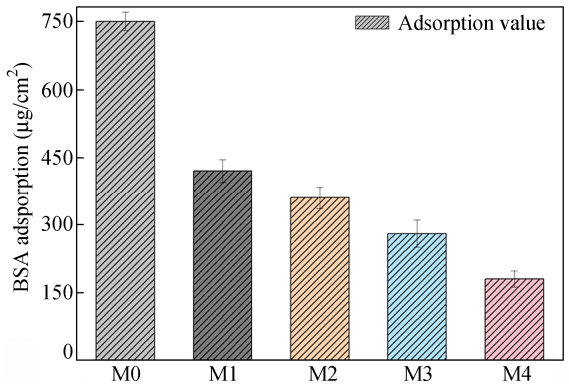


Fig. 10 Amount of BSA adsorbed per unit area of membranes

Dynamic Anti-protein Fouling Property

In the use of membranes, different kinds of liquids flow through the pores dynamically, thus good dynamic anti-organic fouling property and high flux recovery ratio performance for membranes are indispensable[38, 39]. The UF experiments were conducted and the results are shown in Fig. 11. The water flux of PVDF-*g*-PCBMA/Ag membranes decreased with the increasing FD and hydrophilicity and was smaller than that of pure PVDF membrane (M0). The improved hydrophilicity of the membranes could enhance the water permeability by attracting water molecules inside the membrane matrix and facilitating them to pass through the membrane[40]. However, the decreasing pore density and porosity mainly determined the permeation, resulting in the declined fluxes from M2 to M4, as seen clearly in Fig. 6. Interestingly, the FRR of PVDF-*g*-PCBMA/Ag membranes increased with the growing hydrophilicity and was all higher than that of M0, as shown in Fig. 11(a). Additionally, M4 attained the maximum value 93.32%. The results confirmed that AgNPs-PCBMA layer could greatly improve the anti-protein fouling property of PVDF membrane.

More detailed improvements of anti-protein fouling were calculated and the results are shown in Fig. 11(b). Obviously, R_t and R_{ir} decreased, while R_r increased from M0 to M4. The results suggested that the organics on silver fixed PVDF membranes were more easily to clean with water than those on pure and CBMA grafted PVDF membranes. Moreover, M4 obtained the maximum R_r values (70.65%). Additionally, the BSA rejection ratios of PVDF-*g*-PCBMA/Ag membranes were higher than that of pure PVDF membrane and M4 reached the highest of 90.12%.

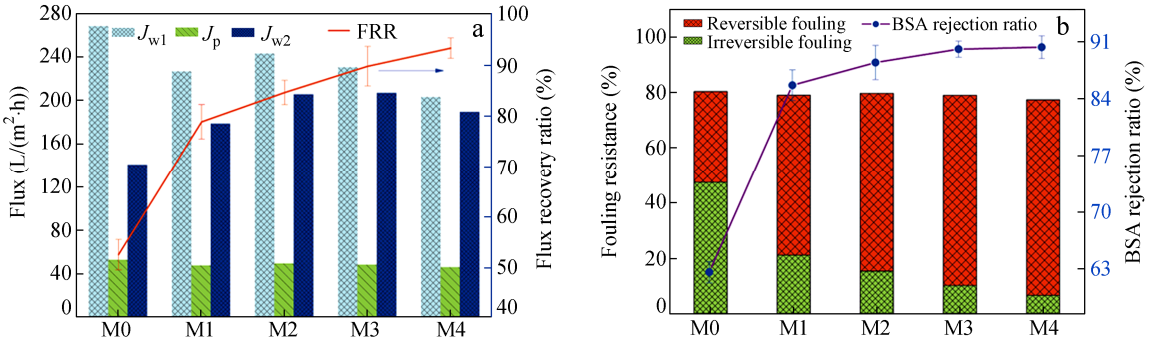


Fig. 11 (a) Water, BSA flux and water flux recovery ratio and (b) fouling resistance ratio of pure PVDF membrane (M0), PVDF-*g*-PCBMA membrane (M1) and PVDF-*g*-PCBMA/Ag membranes (M2–M4)

Durability of the Membranes

To further confirm that whether the PCBMA brushes had been grafted onto the membranes and the stability of the brushes and AgNPs on the membrane surface, durability experiment was performed by measuring the water contact angle of the membrane surface. In Fig. 12, it could be seen from M1 that the initial contact angle gradually increased in 5 days, and without further increase after 10 days. Since the hydrophilicity of the membranes is determined by the PCBMA polymer brush and AgNPs on the membrane surface, this demonstrated that the PCBMA polymer brush was grafted successfully and remained stable on the membrane surface. From M2 to M4, the initial contact angle gradually increased in 10 days, and without further increase after 15 days, which indicated that the AgNPs could also be immobilized stably on the membranes. In summary, the PVDF-*g*-PCBMA/Ag membranes have good stability to use continuously in the water treatment process.

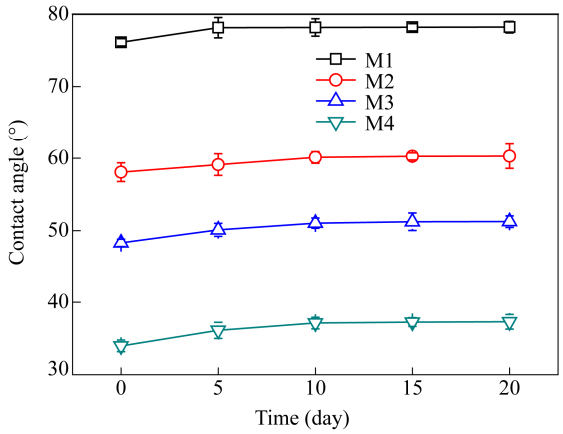


Fig. 12 Time-dependent contact angle of membranes

Synergistic Effect of the PCBMA Polymer Brush and AgNPs on Antibacterial Property of Membranes

The growth of bacteria on surface always decreases the membrane operating life during the practical process. Hence, antimicrobial property of the modified membranes is necessary to be investigated. As shown in Fig. 13, there were no inhibition zones appearing for pure PVDF membrane. However, the zone around PVDF-*g*-PCBMA membrane could be observed clearly, especially for *E. coli*. This led to same conclusion the as the previous papers[25, 26] that the PCBMA polymer brush possessed not only hydrophilicity but also antibacterial properties. The antibacterial activity of the PVDF-*g*-PAA/Ag membrane with the same FD of AgNPs was compared to further demonstrate the antibacterial ability of the PVDF-*g*-PCBMA/Ag membrane. As can be seen from the figure, the PVDF-*g*-PCBMA/Ag membrane exhibited a significant bigger inhibition zone. The result also showed that the PCBMA polymer brush had a certain degree of antimicrobial ability. AgNPs possessed a strong bactericidal property which had already been proved[41, 42]. But compared with pure AgNPs, the antibacterial property of the PVDF-*g*-PCBMA/Ag membrane was greatly enhanced, which further proved that the PCBMA polymer brush and AgNPs had a synergistic effect in terms of antibacterial property. The analysis confirmed that the PVDF membrane after fixing AgNPs on PCBMA layer could obtain a significant anti-bacterial activity toward both negative and positive bacteria. Hydrophilic and anti-fouling protection was formed, which could effectively protect the surface and pores of membrane from being contaminated.

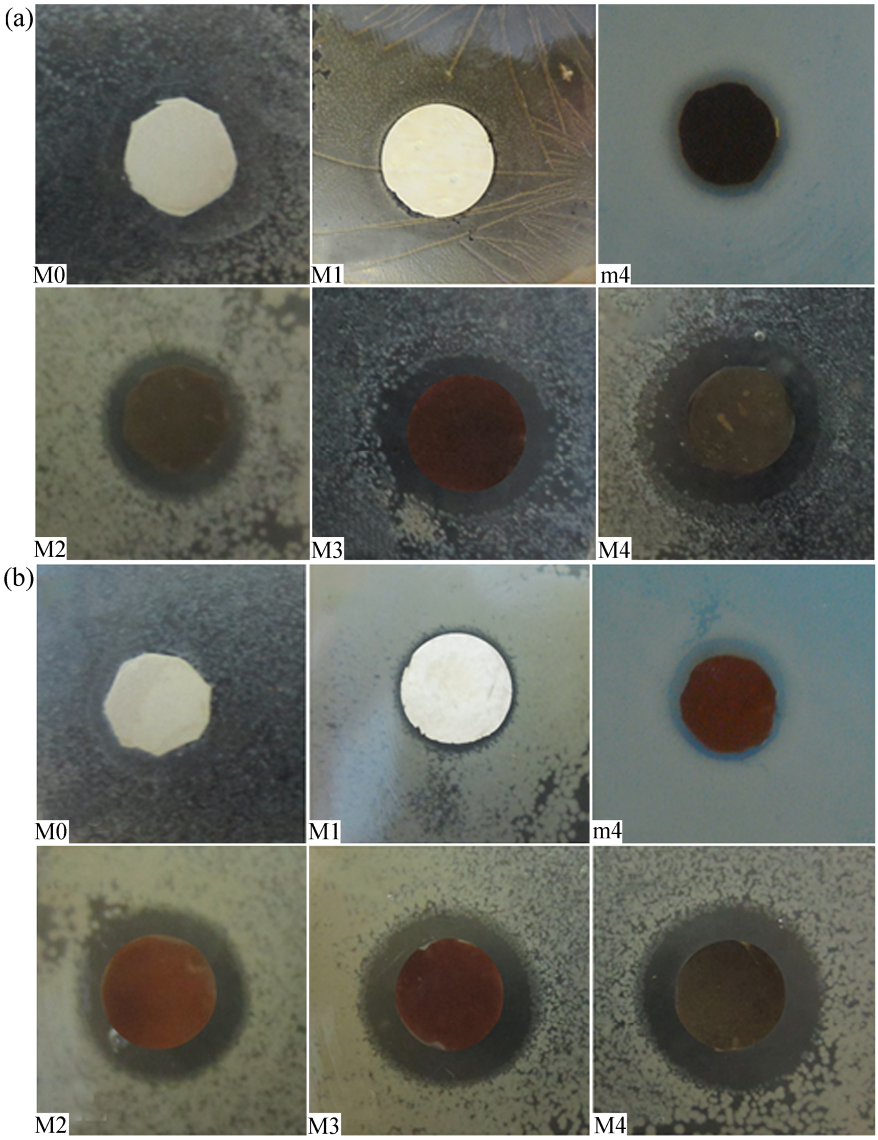


Fig. 13 Antimicrobial performance toward (a) *S. aureus* and (b) *E. coli* of pure PVDF membrane (M0), PVDF-*g*-PCBMA membrane (M1), PVDF-*g*-PAA/Ag membrane (m4) and PVDF-*g*-PCBMA/Ag membranes (M2–M4)

CONCLUSIONS

A novel PVDF-*g*-PCBMA/Ag membrane was successfully fabricated *via* fixing different amounts of AgNPs on the PCBMA brushes. A series of experimental results confirmed that compared with pure AgNPs or the PCBMA polymer brush, the PCBMA/Ag brush provided the PVDF membrane with better hydrophilicity and anti-bacteria performances. Although the decreasing pore density and porosity with the increasing concentration of Ag^+ ions made the flux slightly decline, the AgNPs-PCBMA layer offered the PVDF membrane higher FRR and BSA rejection ratio than those of the pure membrane. In this experiment, zwitterionic PCBMA polymer brushes not only played the role of bridge and also simultaneously increased the anti-protein and anti-bacterial fouling properties. And AgNPs with antibacterial properties also promoted the hydrophilicity of the membrane. In a word, the synergistic effect of PCBMA and AgNPs endowed the PVDF membrane with great improvement of surface property, and a novel method was achieved to prepare super antifouling membranes, which showed a great application for obtaining higher quality water.

REFERENCES

1 Li, J.H., Wang, S.S., Zhang, D.B., Ni, X.X. and Zhang, Q.Q., Chinese J. Polym. Sci., 2016, 34(7): 805
2 Wang, H.J., Feng, H.P., Wang, X.C., Du, Q.C. and Yan, C., Chinese J. Polym. Sci., 2015, 33(6): 823
3 Lee, J.S., Lee, H.H., Seo, J.A., Park, H.S., Park, J. and Min, B.R., Appl. Surf. Sci., 2015, 356: 1207
4 Gomez-Coma, L., Garea, A., Rouch, J.C., Savart, T., Lahitte, J.F., Remigy, J.C. and Irabien, A., J. Membr. Sci., 2016, 498: 218
5 Zhang, X., Lang, W.Z., Yan, X., Lou, Z.Y. and Chen, X.F., J. Membr. Sci., 2016, 499: 179
6 Meng, N., Priestley, R.C.E., Zhang, Y.Q., Wang, H.T. and Zhang, X.W., J. Membr. Sci., 2016, 501: 169
7 Liu, D.P., Li, D., Du, D., Zhao, X.Z., Qin, A., Li, X. and He, C.J., J. Membr. Sci., 2015, 493: 243
8 Qin, A., Li, X., Zhao, X., Liu, D. and He, C., ACS Appl. Mater. Interfaces, 2015, 7: 8427
9 Zhao, X.Z., Xuan, H.X., Chen, Y.L. and He, C.J., J. Membr. Sci., 2015, 494: 48
10 Wang, L., Pan, K., Li, L. and Cao, B., Ind. Eng. Chem. Res., 2014, 53: 6401
11 Yang, X., He, Y., Zeng, G.Y., Zhan, Y.Q., Pan, Y., Shi, H. and Chen, Q., J. Membr. Sci., 2016, 51: 8965
12 Xiao, Y., Liu, X.D., Wang, D.X., Lin., Y.K., Han, Y.P. and Wang, X.L., Desalination, 2013, 313: 16
13 Baghbanzadeh, M., Rana, D., Matsuura, T. and Lan, C.Q., Desalination, 2015, 369: 75
14 Zhang, Y., Chen, Y., Zhang, H., Zhang, B. and Liu. J., J. Inorg. Biochem, 2013, 118: 59
15 Huang, L.C., Zhao, S., Wang, Z., Wu, J.H., Wang, J.X. and Wang, S.C., J. Membr. Sci., 2016, 499: 269
16 Zhang, M., Zhang, K.S., Gusseme, B.D. and Verstraete, W., Water Res., 2012, 46: 2077
17 Sawada, I., Fachrul, R., Ito, T., Ohmukai, Y., Maruyama, T. and Matsuyama, H., J. Membr. Sci., 2012, 387: 1
18 Liu, Y.L., Rosenfield, E., Hu, M. and Mi, B.X., Water Res., 2013, 47: 2949
19 Shi, H.Y., Liu, F. and Xue, L.X., J. Membr. Sci., 2013, 437: 205
20 Chen, Y.F, Zhang, Y.T., Zhang, H.Q., Liu, J.D. and Song, C.H., Chem. Eng. J., 2013, 228: 12
21 Wang, P.P., Ma, J., Wang, Z.H., Shi, F.G. and Liu, Q.L., Langmuir, 2012, 28: 4776
22 Zhang, G.L., Lu, S.F., Zhang, L., Meng, Q., Shen, C. and Zhang, J.W., J. Membr. Sci., 2013, 436: 163
23 Li, J.H., Shao, X.S., Zhou, Q., Li, M.Z. and Zhang, Q.Q., Appl. Surf. Sci., 2013, 265: 663
24 Yin, J., Yang, Y., Hu, Z.Q. and Deng, B.L., J. Membr. Sci., 2013, 441: 73
25 Zhao, Y.F., Zhu, L.P., Yi, Z., Zhu, B.K. and Xu, Y.Y., J. Membr. Sci., 2013, 440: 40
26 Huang, C.J., Li, Y.T. and Jiang, S.Y., Anal. Chem., 2012, 84: 3440
27 Cheng, G., Li, G.Z., Xue, H., Chen, S.F., Bryers, J.D. and Jiang, S.Y., Biomaterials, 2009, 30: 5234
28 Hu, R., Li, G.Z., Jiang, Y.J., Zou, J.J., Wang, L. and Zhang, X.W., Langmuir, 2013, 29: 3773
29 Li, M.Z., Li, J.H., Shao, X.S., Miao, J., Wang, J.B., Zhang, Q.Q. and Xu, X.P., J. Membr. Sci., 2012, 405: 141
30 Zhang, Z., Chen, S.F. and Jiang, S.Y., Biomacromolecules, 2006, 7: 3311
31 Maximous, N., Nakhla, G., Wan, W. and Wong, K., J. Membr. Sci., 2010, 352: 222
32 Zhang, J.G., Xu, Z.W., Mai, W., Min, C.Y., Zhou, B.M., Shan, M.J., Li, Y.L., Yang, C.Y., Wang, Z. and Qian, X.M., J. Mater. Chem. A., 2013, 1: 3101
33 Liu, X., Qi, S., Li, Y., Yang, Y., Cao, B. and Tang, Y.Y., Water Res., 2013, 47: 3081
34 Enomoto, R., Sato, M., Fujii, S., Hirai, T., Takahara, A. and Ishihara, K.S., J. Polym. Sci., Part A: Polym. Chem., 2014, 52: 2822
35 Kumar, M. and Ulbricht, M., RSC Adv., 2013, 3: 12190
36 Liu, J.Y. and Hurt, R.H., Int. J. Environ. Sci. Technol., 2010, 44: 2169
37 Zhou, Q., Li, J.H., Yan, B.F., Wu, D. and Zhang, Q.Q., Chinese J. Polym. Sci., 2014, 32(7): 892
38 Qin, J.X., Lin, S.S., Song, S.Q., Zhang, L. and Chen, H.L., ACS. Appl. Mater. Interfaces, 2013, 5: 6649
39 Sinha, M.K. and Purkait, M.K., J. Membr. Sci., 2013, 437: 7
40 Meng, J., Song, L., Xu, H., Kong, H., Wang, C., Guo, X. and Xie, S., Nanomedicine, 2005, 1: 136
41 Mijnendonckx, K., Leys, N., Mahillon, J., Silver, S. and Houdt. R.V., BioMetals, 2013, 26: 609
42 Zhu, X., Bai, R., Wee, K., Liu, C. and Tang, S., J. Membr. Sci., 2010, 363: 278